Slowing down of fast electrons as probe for charging and decharging dynamics of ion-irradiated insulators

E. De Filippo,[1] G. Lanzanó,[1,*] F. Amorini,[2] E. Geraci,[1,3] L. Grassi,[1,3] E. La Guidara,[1,4] I. Lombardo,[2,5] G. Politi,[1,3] F. Rizzo,[2,3] P. Russotto,[2,4] C. Volant,[6] S. Hagmann,[7,8] and H. Rothard[9,†]

[1]*Istituto Nazionale di Fisica Nucleare Sezione di Catania, Via S. Sofia 64, I-95123 Catania, Italy*

[2]*Istituto Nazionale di Fisica Nucleare-Laboratori Nazionali del Sud, LNS, Via S. Sofia 62, I-95123 Catania, Italy*

[3]*Dipartimento di Fisica e Astronomia, Via S. Sofia 64, I-95123 Catania, Italy*

[4]*Centro Siciliano Fisica Nucleare e Struttura della Materia, CSFNSM, Catania, Italy*

[5]*Facoltà di Ingegneria ed Architettura, Università degli Studi di Enna "Kore," Enna, Italy*

[6]*Département Astrophysique, Physique des Particules, Physique Nucléaire et de l'Instrumentation Associée/Service de Physique Nucléaire, CEA/Saclay, F-91191 Gif-sur-Yvette, France*

[7]*GSI Helmholtzzentrum für Schwerionenforschung, D-64291 Darmstadt, Germany*

[8]*Institut für Kernphysik IKF, J. W. Goethe Universität, Frankfurt am Main, Germany*

[9]*Centre de Recherche sur les ions, les Matériaux et la Photonique, CIMAP-CIRIL-Ganil (CEA/CNRS/ENSICAEN/Université de Caen-Basse Normandie), BP 5133, F-14070 Caen Cedex 05, France*

(Received 7 April 2011; published 15 June 2011)

The slowing down of fast electrons emitted from insulators [Mylar, polypropylene (PP)] irradiated with swift ion beams (C, O, Kr, Ag, Xe; 20–64 MeV/u) was measured by the time-of-flight method at LNS, Catania and GANIL, Caen. The charge buildup, deduced from both convoy- and binary-encounter electron peak shifts, leads to target material-dependent potentials (6.0 kV for Mylar, 2.8 kV for PP). The number of projectiles needed for charging up (charging-up time constant) is inversely proportional to the electronic energy loss. After a certain time, a sudden decharging occurs. For low beam currents, charging-up time, energy shift corresponding to maximum charge buildup, and time of decharging are regular. For high beam currents, the time intervals become irregular (chaotic).

DOI: 10.1103/PhysRevA.83.064901 PACS number(s): 34.35.+a, 34.50.Fa, 79.20.−m

I. INTRODUCTION

Irradiation of insulators with ion beams may lead to charging up due to both the injected charge of the projectile and the emission of low-energy secondary electrons (see Ref. [1] and references therein). For the past few years, guiding phenomena in nanocapillaries with the possible application of nanofocused beams have been extensively studied (see Refs. [2–4], and references therein). To control this phenomenon, a refined understanding of ion-induced charging and decharging dynamics is necessary [4]. This is true both for slow (keV) multiply charged ions and swift ($\geqslant$MeV) ion beams. In this latter domain of high projectile velocity, first applications (single-cell irradiation with microcapillary focused beams) emerge [5].

In Ref. [1], we reported results on the ion irradiation-time-dependent slowing down of fast binary-encounter electrons (BEEs) emitted from the insulating polymers Mylar and polypropylene (PP). All of the experiments were performed with the multidetector ARGOS. The charging-up-induced BEE energy shift ΔE_{BEE} and the projectile-dependent charging-up time constant were measured in a direct and clear-cut way. Here, as a short follow-up to Ref. [1], we report further results on BEE emission, and an analysis of convoy electron (CE) emission, which complements the BEE data. Indeed, the CE data allow for an independent control of the BEE results. Also, considering both data sets, a wider range of projectile energies can be accounted for (see below).

II. MEASUREMENT OF ELECTRON VELOCITY DISTRIBUTIONS

Experimental details have been described in Ref. [1]. Beams of highly charged C (23 and 40 MeV/u), O (23 MeV/u), Kr(64 MeV/u), Ag (40 MeV/u), and Xe (20, 23, and 30 MeV/u) ions were used to irradiate thin foils at the superconducting cyclotron of LNS, Catania and at GANIL, Caen. The multidetector ARGOS [1,6–8] was mounted in the large scattering chamber CICLOPE or the CHIMERA chamber of LNS, or in the NAUTILUS chamber at GANIL. The velocity of fast electrons was measured by the time-of-flight (TOF) method with scintillation detectors. The experimental and calibration procedures are described in detail in Ref. [1]. An example of spectra is shown in Fig. 1; the inset shows a sketch of the experimental setup. The beam traverses the target foils and the beam current I_{beam} is measured in a Faraday cup. When possible, the beam current was varied over orders of magnitude, in the range from approximately 2 pA $\leqslant I_{\mathrm{beam}} \leqslant$ 350 pA, depending on the beam. The beam diameter ϕ on the target was 2 mm $\leqslant \phi \leqslant$ 3 mm. The targets were mounted free-standing as a "sandwich" between two thin rectangular metal frames (40 mm × 15 mm). In the case of targets with thin Au layers, this assured electrical contact with the target holder, which could hold up to 12 of these target frames. The size of the oval hole in the frames (through which the beam passed in the center, crossing the free-standing targets), was

*Deceased.
†rothard@ganil.fr

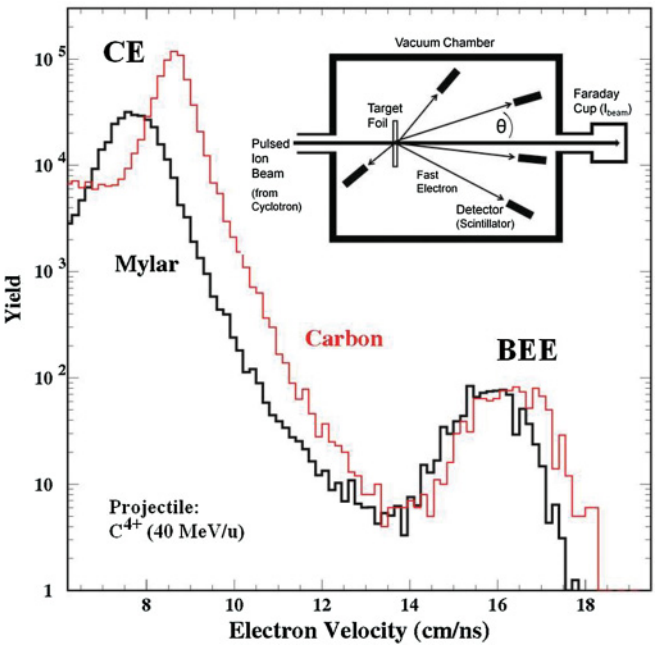

FIG. 1. (Color online) Forward electron velocity spectra from a C foil (conductor) and a Mylar target (insulator) irradiated by C^{4+} (40 MeV/u). Observation angle $\theta = 2^\circ$. The inset shows a schematic drawing of the experimental setup.

10 mm × 15 mm in most cases. The data used here were taken with detectors mounted close to observation angles of $1.8^\circ \leqslant \theta \leqslant 9.2^\circ$. The residual pressure was $\sim 10^{-6}$ mbar or lower.

Targets included conducting C foils ($\approx 100\ \mu g/cm^2$), insulating Mylar ($\approx 100\ \mu g/cm^2$), PP (4 μm), and in some cases, Au-My-Au sandwich targets (My of $\approx 100\ \mu g/cm^2$ thickness, covered with a thin Au layer of $\approx 10\ \mu g/cm^2$ on both surfaces), as well as Au-My foils (My covered with a thin Au layer of $\approx 10\ \mu g/cm^2$ on one surface). The gold-coated surface was directed in the forward direction (on the exit side of the ion beam and of the fast electrons). The single-side layers and double-side layers were produced in the same evaporation setup at LNS, before each of the experiments. Such single-layer and sandwich targets were used in four beam times (2004, 2007, 2009) in three different large vacuum chambers (see above) both at GANIL and LNS.

Figure 1 shows electron velocity distributions at an ejection angle of $\theta = 2^\circ$ for C^{4+} (40 MeV/u) impact on a conducting carbon target and on an insulating Mylar target. Two distinct structures can be observed. BEEs appear at approximately twice the projectile velocity [1,7–10]. They stem from a knock-on ionization of target electrons by the projectile nucleus (scattering of a target electron in the projectile's Coulomb field). The initial peak width is given by the "Compton profile" of the bound target electrons. The observed peak is broadened due to transport effects, i.e., elastic and inelastic scattering of the electrons on their way from the point of ionization to the target surface [9,10]. CEs originate from (target) electron capture or (projectile) electron loss to low-lying projectile continuum states. They have kinetic energies close to zero in the projectile frame and thus travel with the same velocity as the projectile [6–9].

For projectiles with velocities below a threshold situated at ~25 MeV/u, only BEEs can be analyzed with sufficient precision [1]; after charging-up-induced slowing down, the energy of the CE falls below this energy threshold. On the other hand, above ~50 MeV/u, the analysis of BEEs is impossible, since the time resolution becomes too small for such fast electrons. Therefore, if both data for CE and BEE ejection are analyzed, charging-up phenomena can be studied over a wider range of projectile energy ranges. As can be seen from Fig. 1, the charging up of the Mylar foil leads to a shift of the CE and the BEE peaks toward lower velocities than observed with the conducting C foil. This is due to slowing down of the electrons due to buildup of a positive charge. Also, a broadening is observed for the CE peak, which can be possibly related to electron transport phenomena [9,10].

III. CHARGING AND DECHARGING DYNAMICS

For quantitative analysis of the data, the same statistical method as reported in Ref. [1] is applied to both the CE and BEE peaks: (i) CE or BEE electrons are separated from the background by choosing an appropriate window in the "deposited energy–time-of-flight" bidimensional plot (Fig. 2 of Ref. [1]). (ii) The elapsed time during one run is divided in intervals Δt. The choice of the most appropriate Δt depends on the acquired statistics in this time interval, and is of the order of $1\ s \leqslant \Delta t \leqslant 100\ s$, depending on the beam properties (projectile, current). (iii) Over each interval Δt, the mean time of flight ($\langle TOF \rangle$) of BEE and CE is calculated and plotted as a function of irradiation time. Figure 2 shows the $\langle TOF \rangle$ of CE emitted from Mylar bombarded by C^{4+} (40 MeV/u) beams at three different ion beam currents $I_{beam} = 8.5$, 75, and 330 pA.

The $\langle TOF \rangle$ increases in all cases with irradiation time. Thus, an attractive force from an electric field corresponding to a positive charging up leads to a slowing down of CE and BEE. The $\langle TOF \rangle$ continues to rise and converges toward a value for "infinite" times $\langle T(\infty) \rangle$. However, after a certain time, a sudden decharging (charge breakdown) occurs. For very low beam currents, this phenomenon seems to be quite regular: the charging-up time, the potential corresponding to the maximum charge buildup, and the time at which decharging occurs are well reproduced [Fig. 2(a)]. With increasing beam current, time intervals and buildup potentials become increasingly irregular and chaotic [Figs. 2(b) and 2(c)]. With the highest beam currents, in most cases charge breakdown occurs before complete charging up was obtained, i.e., before $\langle TOF \rangle$ gets close to the limit $\langle T(\infty) \rangle$ [Fig. 2(c)].

For low enough beam currents, where the $\langle TOF \rangle$ values come close to the limit $\langle T(\infty) \rangle$, the increase of the TOF of CE (and BEE) follows an exponential increase with a certain charging-up time constant τ:

$$\langle TOF \rangle(t) = \langle T(\infty) \rangle [1 - \exp(-t/\tau)]. \quad (1)$$

In contrast, with a conducting C foil the $\langle TOF \rangle$ remains constant, since electronic relaxation is very fast in conductors (of the order of fs), whereas in insulators the relaxation time may be much longer. The time constant τ depends on the ion beam current, as can be seen from Fig. 2, but not on the number of accumulated projectiles; no dose effect is observed. As already reported in Ref. [1], charging up of PP is faster than that

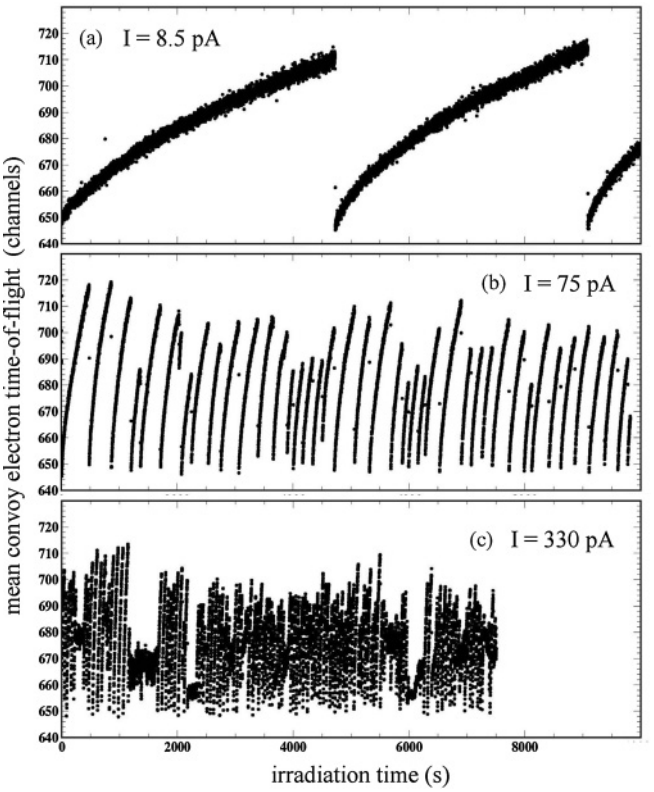

FIG. 2. Mean TOF of CE induced by C^{4+} (40 MeV/u) as a function of irradiation time t (target: Mylar) at three different ion beam currents of 8.5, 75, and 330 pA.

of Mylar, but the absolute value of the resulting final electrical field is lower for PP. A single Au layer at the CE, BEE, and ion beam exit surface strongly suppresses the slowing down. Surprisingly, with Au-Mylar-Au sandwich targets, charging up occurs and closely resembles that of the pure insulator Mylar. This may be a hint for a contribution from a bulk phenomenon in addition to surface charging up. Xiao *et al.* [11] observed a shift of the CE energy with polymer foils due to the nuclear track potential induced in the wake of the heavy ion.

IV. DEPENDENCE ON THE ELECTRONIC ENERGY LOSS

Our experiments were performed with several swift ion beams in a large range of dE/dx values. Two orders of magnitude were covered, from $dE/dx \approx 0.47$ keV μg^{-1} cm^2 to $dE/dx \approx 54$ keV μg^{-1}cm^2. This allows studying the dependence of the charging up on the amount of energy deposited in the target by electronic energy loss (inelastic interaction with the target electrons). As observables for the charging dynamics, we first use the number N of accumulated projectiles needed to charge up the target, which can be calculated from the charging time constant τ of the exponential function of Eq. (1) [1]. A second quantity is the electron peak energy shifts ΔE with respect to the energy observed with a conducting C foil of comparable thickness [1]. The energy shifts for BEE, ΔE_{BEE}, and for CE, ΔE_{CE}, should be equal to the induced slowing-down potential.

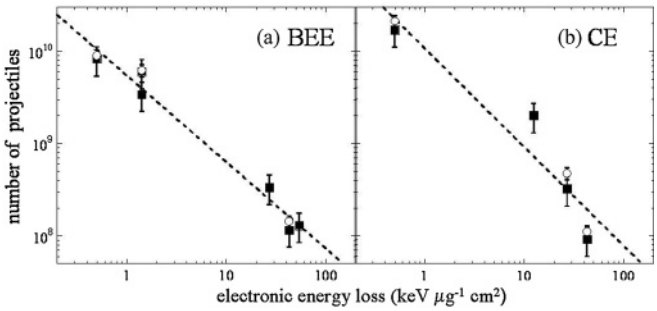

FIG. 3. Accumulated number N of projectiles corresponding to the charging-up time constant τ of Eq. (1) as a function of the electronic energy loss in the target (Mylar: full squares; Au-Mylar-Au: open circles). The lines are fits of a power law $\sim (dE/dx)^n$ to the Mylar data (see text): (a) binary-encounter electrons (BEE), (b) convoy electrons (CE).

Figure 3 shows N as a function of the energy loss dE/dx, which was calculated with the widely used SRIM software [12] as obtained with BEE [Fig. 3(a), same as Fig. 8(a) of Ref. [1], here enriched with additional data] and with CE [Fig. 3(b)]. A power law is observed in both cases, $N \sim (dE/dx)^n$, with the exponent $n(\mathrm{BEE}) = -(0.94 \pm 0.07)$ for BEE and $n(\mathrm{CE}) = -(1.07 \pm 0.08)$.

N is thus found to be inversely proportional to dE/dx, since the charging buildup is mainly related to low-energy secondary electron emission. The yield of secondary electrons was observed to be roughly proportional to the electronic energy loss dE/dx of the projectile [9].

The peak shifts ΔE_{BEE} and ΔE_{CE} are plotted as functions of the electronic energy loss in Figs. 4(a) and 4(b). The mean value for the observed BEE and CE peak shifts ($\Delta E \approx 6.0$ kV) are in good agreement for both CE and BEE data sets. No dependence on dE/dx is observed. ΔE_{BEE} depends on the target material: $\Delta E \approx 6.0$ kV for Mylar, and $\Delta E \approx 2.8$ kV for PP. The results reported here confirm and extend those of Ref. [1]. Sandwich targets with gold layers on both surfaces behaved in the same way as pure insulators, whereas a single gold layer screened the outgoing electron. The question whether the observed charging up is a surface

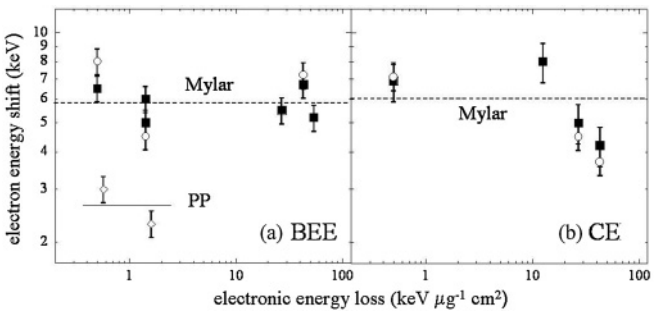

FIG. 4. (a) Binary-encounter–electron peak shift ΔE_{BEE} as a function of electronic energy loss in the target, for Mylar (full squares), Au-My-Au sandwich targets (open circles), and polypropylene (open diamonds). (b) Convoy electron peak shift ΔE_{CE} as a function of electronic energy loss in the target, for Mylar (full squares) and Au-My-Au sandwich targets (open circles). The dotted lines represent the mean values of all data points.

or a bulk (track) phenomenon, or if both processes contribute, remains open and is the subject of further investigations.

ACKNOWLEDGMENTS

Special thanks to the LNS-CS and GANIL staff for providing excellent ion beams. Thanks to N. Giudice, A. Grimaldi, N. Guardone, V. Sparti, and S. Urso from INFN Sez. Catania; V. Campagna, G. De Luca, A. Di Stefano, and A. Salomone from INFN-LNS; J. Cacitti and R. Beunard from GANIL for technical assistance; and to C. Marchetta, and E. Costa for target preparation. Three of us (S.H., H.R., and C.V.) would like to thank their Sicilian colleagues for their great hospitality and INFN for financial support.

[1] E. De Filippo *et al.*, Phys. Rev. A **82**, 062901 (2010).
[2] K. Schiessl, W. Palfinger, K. Tökési, H. Nowotny, C. Lemell, and J. Burgdörfer, Phys. Rev. A **72**, 062902 (2005).
[3] Y. Kanai, M. Hoshino, T. Kambara, T. Ikeda, R. Hellhammer, N. Stolterfoht, and Y. Yamazaki, Phys. Rev. A **79**, 012711 (2009).
[4] N. Stolterfoht, R. Hellhammer, Z. Juhász, B. Sulik, V. Bayer, C. Trautmann, E. Bodewits, A. J. de Nijs, H. M. Dang, and R. Hoekstra, Phys. Rev. A **79**, 042902 (2009).
[5] Y. Iwai, T. Ikeda, T.M. Kojima, Y. Yamazaki, K. Maeshima, N. Imamoto, T. Kobayashi, T. Nebiki, T. Narusawa, and G. P. Pokhil, Appl. Phys. Lett. **92**, 023509 (2008).
[6] G. Lanzanò, E. De Filippo, M. Geraci, A. Pagano *et al.*, Nucl. Phys. A **683**, 566 (2001).
[7] E. De Filippo *et al.*, Phys. Rev. A **68**, 024701 (2003).
[8] E. De Filippo, G. Lanzanò, H. Rothard, and C. Volant, Phys. Rev. Lett. **100**, 233202 (2008).
[9] H. Rothard and B. Gervais, Mat. Fys. Medd. Dan. Vid. Selsk. **52**, 497 (2006).
[10] H. Rothard, G. Lanzanò, D. H. Jakubassa-Amundsen, E. De Filippo, and D. Mahboub, J. Phys. B **34**, 3261 (2001).
[11] G. Xiao, G. Schiwietz, P. L. Grande, N. Stolterfoht, A. Schmoldt, M. Grether, R. Köhrbrück, A. Spieler, and U. Stettner Phys. Rev. Lett. **79**, 1821 (1997).
[12] J. F. Ziegler, J. P. Biersack, and U. Littmark, *The Stopping and Range of Ions in Solids* (Pergamon, New York, 1985) (new edition in 2009), [www.srim.org.]